

Stereochemistry of the Furan–Maleic Anhydride Cycloaddition: A Theoretical Study

Saturnino Calvo-Losada

Departamento de Química Física, Universidad de Málaga
Campus de Teatinos, 29071 Málaga, Spain

Dimas Suárez*,†

Department of Chemistry, Eberly College of Sciences
The Pennsylvania State University, 152 Davey Laboratory
University Park, Pennsylvania 16802-6300

Received April 22, 1999

Revised Manuscript Received September 27, 1999

One of the most important aspects of the Diels–Alder reactions is the understanding of the factors influencing the endo/exo stereoselectivity.¹ To analyze the origin of the Diels–Alder stereoselectivity, the [4+2] cycloaddition of furan and maleic anhydride has been studied experimentally for many years as an interesting model system.^{2–5}

Woodward and Baer showed that the crystalline product from the title reaction has the exo stereochemistry.² In pioneering NMR research,³ Anet investigated the kinetics of the process in acetonitrile solution reporting that the exo isomer is initially formed twice as fast as the endo isomer at room temperature. However, the endo compound initially formed reverses into reactants easily whereas the exo cycloaddition gives a relatively stable adduct, then being the product of thermodynamic control. Since the kinetically favored formation of Diels–Alder exo compounds constitutes an exception to the well-known rule of predominant endo addition, Lee and Herndon reinvestigated the title reaction using NMR spectroscopy.⁴ According to these authors, the rate constant for the formation of the endo adduct in acetonitrile solution at 40 °C is almost 500 times larger than that of the exo adduct. However, the NMR results of Koreshkov et al.⁵ indicate that the rate of formation of the exo isomer is very close to that of the endo one at both normal and high pressures. Very recently, NMR experiments carried out by González and López-Ortiz have determined that the activation energy for the formation of the endo adduct is only 0.20 kcal/mol below that of the exo adduct.⁶

To complement experimental results on the assignment of the endo/exo kinetic preference, a quantum-chemical investigation of the title reaction is reported in this work. Moreover, further insight into the origin of the stereoselectivity of the Diels–Alder reactions can be gained.

Molecular geometry optimizations followed by analytical frequency calculations were performed at the MP2/6-31G* and

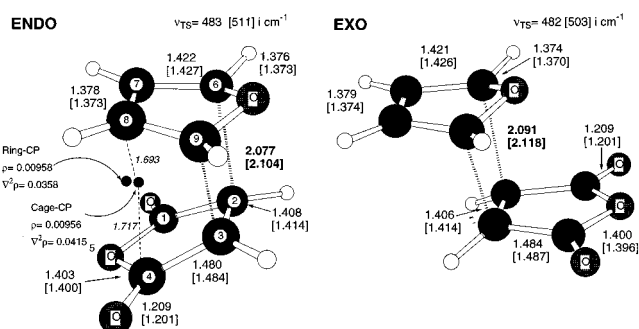


Figure 1. Molecular geometries of the TSs for the Diels–Alder addition between furan and maleic anhydride. MP2/6-31G* and [B3LYP/6-31G*] bond distances in Å. Ring critical point (CP) and cage-CP located on the C_s symmetry plane in the MP2/6-31G* charge density of the endo TS are also shown. CP properties are given in au.

B3LYP/6-31G* levels of theory^{7,8} using the Gaussian 94 and Gaussian 98 suites of programs.⁹ MP2 and B3LYP single-point energy calculations using the 6-311+G(3df,2p) basis set were also carried out on the corresponding MP2/6-31G* and B3LYP/6-31G* geometries, respectively. In addition, MP4/6-31G*/MP2/6-31G* calculations were done to estimate the effect of more elaborated N -electron treatments on the calculated relative energies.¹⁰

We see in Figure 1 that the MP2 and B3LYP methods render very similar geometries and imaginary frequencies for the endo and exo transition structures (TSs). Addition of the MP2/6-31G* thermal corrections to a combination of the MP4 and MP2 electronic energies¹¹ renders activation Gibbs energies of 21.67 and 22.23 kcal/mol for the endo and exo TSs, respectively. The B3LYP Gibbs energy barriers are 36.0 kcal/mol for both the endo and exo TSs, around 14 kcal/mol above the MPn-based ΔG values (see Table 1).

All the levels of theory used in this work reproduce the thermodynamic preference for the formation of the exo stereoisomer observed experimentally.^{3–5} Thus, the endo and exo adducts have MPn-based ΔG_{rxn} values in the gas phase of 1.85 and -0.02 kcal/mol, respectively, while the B3LYP ΔG_{rxn} calculations predict that the exo isomer is 16.44 kcal/mol above reactants and 2.77 kcal/mol more stable than the endo adduct.

Since we are mainly interested in the stereochemical outcome of the furan–maleic anhydride cycloaddition, we will focus hereafter on the endo/exo kinetic aspects of the process. In this sense, the structural data of TSs hardly depend on the endo–exo orientation of the TSs (see Figure 1). Furthermore, both TSs have an identical furan \rightarrow maleic anhydride Mulliken charge transfer of 0.23 (MP2/6-31G*) and 0.24 e (B3LYP/6-31G*). Using the Bader's theory of atoms in molecules,¹² the charge density $\rho(\vec{r})$

(7) Hehre, W. J.; Radom, L.; Pople, J. A.; Schleyer, P. v. R. *Ab Initio Molecular Orbital Theory*; John Wiley & Sons Inc.: New York, 1986.

(8) (a) Becke, A. D. *J. Chem. Phys.* **1993**, *98*, 5648. (b) Becke, A. D. *Phys. Rev. B* **1988**, *38*, 3098. (c) Lee, C.; Yang, W.; Parr, R. G. *Phys. Rev. B* **1988**, *37*, 785.

(9) (a) Frisch, M. J. et al. *Gaussian 94*; Gaussian, Inc.: Pittsburgh, PA, 1995. (b) Frisch, M. J. et al. *Gaussian 98*; Gaussian, Inc.: Pittsburgh, PA, 1998.

(10) Due to computational shortcomings, QCISD(T) or CCSD(T) energies were not obtained for the furan + maleic anhydride reaction. Nonetheless, we note that the MP4/6-31G*/MP2/6-31G* electronic energies for the energy barrier (22.3 kcal/mol) and reaction energy (-42.3 kcal/mol) of the 1,3-butadiene + ethylene Diels–Alder reaction compare reasonably well with those at QCISD(T)/6-31G*/MP2/6-31G* (25.0 and -40.6 kcal/mol, respectively).

(11) Composite electronic energies were obtained following the usual additive procedure: $E_{\text{MP4/6-311+G(3df,2p)}} \approx E_{\text{MP4/6-31G*}} + E_{\text{MP2/6-311+G(3df,2p)}} - E_{\text{MP2/6-31G*}}$.

(12) Bader, R. F. W. *Atoms in Molecules. A Quantum Theory*; Clarendon Press: Oxford, 1990.

† On leave from Departamento de Química Física y Analítica, Universidad de Oviedo, Spain.

(1) (a) Carruthers, W. *Cycloaddition Reactions in Organic Synthesis*; Pergamon Press: New York, 1990. (b) Sauer, J.; Sustmann, J. *Angew. Chem., Int. Ed. Engl.* **1980**, *19*, 779.

(2) Woodward, R. B.; Baer, H. *J. Am. Chem. Soc.* **1948**, *70*, 1161.

(3) Anet, F. A. L. *Tetrahedron Lett.* **1962**, 1219.

(4) Lee, M. W.; Herndon, W. C. *J. Org. Chem.* **1978**, *43*, 516.

(5) (a) Zhulin, V. M.; Bogdanov, V. S.; Keltseva, M. V.; Kabotyanskaya, E. B.; Koreshov, Y. D. *Bull. Acad. Sci. USSR D. Chem. Sci.* **1989**, *38*, 2303. (b) Zhulin, V. M.; Keltseva, M. V.; Bogdanov, V. S.; Koreshov, Y.; Kabotyanskaya, E. B. *Bull. Acad. Sci. USSR D. Chem. Sci.* **1990**, *39*, 456.

(6) The kinetics of the reaction of furan with maleic anhydride, in deuterated acetonitrile, at 273 K, was studied by 400 MHz ¹H NMR, following the evolution of the integrals corresponding to the hydrogens α to the oxygen bridge of the endo (5.43 ppm) and exo (5.34 ppm) [4+2] adducts. According to these results, the endo adduct is formed slightly faster than the exo one, resulting in a difference in the activation energy of 0.20 kcal/mol, which seems to be in sharp disagreement with the previous results of Lee and Herndon in ref 4 (personal communication from F. J. González).

Table 1. Relative Energies and Gibbs Energies (kcal/mol) with Respect to Reactants of the TSs and Adducts for the Diels–Alder Addition between Furan and Maleic Anhydride

structures	MP2/ 6-31G*	MP2/ 6-311+G(3df,2p) ^a	MP4/ 6-31G* ^a	B3LYP/ 6-31G*	B3LYP/ 6-311+G(3df,2p) ^b	$\Delta G_{\text{gas phase}}^c$	$\Delta\Delta G_{\text{solvation}}^d$	$\Delta G_{\text{solution}}^e$
TS endo	6.13	2.12	10.46	18.39	22.37	21.67 (35.96)	−2.41	19.26
TS exo	6.46	2.77	10.68	18.34	22.37	22.23 (35.97)	−2.72	19.51
endo adduct	−17.28	−17.61	−16.09	−3.46	2.63	1.85 (18.99)	−2.08	−0.23
exo adduct	−19.82	−19.25	−18.69	−6.00	0.10	−0.02 (16.44)	−2.78	−2.80

^a Single-point calculations on the MP2/6-31G* geometries. ^b Single-point calculations on the B3LYP/6-31G* geometries. ^c 1 bar, 298.15 K. Thermal corrections from MP2/6-31G* frequencies and MPn composite electronic energies. Values in parentheses correspond to the B3LYP/6-311+G(3df,2p)/B3LYP/6-31G* electronic energies with B3LYP/6-31G* thermal corrections. ^d Single-point MP2/6-31G* PCM-UAHF calculations on the MP2/6-31G* geometries. ^e $\Delta G_{\text{solution}} = \Delta G_{\text{gas phase}} + \Delta\Delta G_{\text{solvation}}$.

was further analyzed locating a set of critical points on $\rho(\vec{r})$ which satisfy the Poincaré–Hopf relationship (nuclei – bonds + rings – cages = 1). Inspection of both the MP2/6-31G* and B3LYP/6-31G* bond critical point properties does not reveal any clear distinction between the endo and exo $\rho(\vec{r})$. However, at the MP2/6-31G* level, with respect to the exo $\rho(\vec{r})$, the endo $\rho(\vec{r})$ has an additional ring critical point and a cage critical point (a local minimum of $\rho(\vec{r})$) located on the C_s symmetry plane and situated in an intermediate position between the C_1 – C_7 and C_4 – C_8 atoms (see Figure 1).¹³ Although the C_1 – C_7 and C_4 – C_8 contacts in the endo TS pass from 2.964 Å at B3LYP/6-31G* to 2.858 Å at MP2/6-31G*, the various analyses here reported suggest that the C_1 – C_7 and C_4 – C_8 through-space interactions do not correspond to a secondary diene \rightarrow dienophile charge delocalization. This seems to be in contrast with the common interpretation of the “maximum accumulation of unsaturations” rule of Alder in terms of classical secondary orbital interactions.¹⁴

MPn methods predict a small endo kinetic preference, which ranges from 0.22 (MP4/6-31G*/MP2/6-31G*) to 0.65 kcal/mol (MP2/6-311+G(3df,2p)/MP2/6-31G*), whereas the B3LYP method renders endo/exo TSs which are practically isoenergetic. Previous computational experience¹⁵ has shown that, in contrast with conventional ab initio calculations, most of the present density functional methods including the B3LYP functional do not cover the dispersion energy and render purely repulsive interactions for prototypical van der Waals systems.¹⁶ Therefore, based on the comparative analyses between MPn and B3LYP results, it seems reasonable to assign the kinetic endo preference to the effect of dispersion interactions favoring the endo orientation through π – π contacts.^{17,18} The dependence on the basis set of the endo preference observed in the MP2 energies is most probably due to the inclusion of diffuse outer functions which are known to have a large influence on the calculation of molecular properties and dispersion interactions.¹⁹

To take into account condensed-phase effects on the kinetics and thermodynamics of the title reaction, solvation Gibbs energies $\Delta G_{\text{solvation}}$ in acetonitrile solution were computed using the UAHF (united atom Hartree–Fock) parametrization²⁰ of the polarizable continuum model²¹ (PCM) including both electrostatic and

nonelectrostatic solute–solvent interactions. Single-point MP2/6-31G* PCM-UAHF calculations on the MP2/6-31G* gas-phase geometries render relative solvation energies ($\Delta\Delta G_{\text{solvation}}$) with respect to separate reactants of −2.41 and −2.72 kcal/mol for the endo and exo TSs, respectively (see Table 1). Although the MP2/6-31G* dipole moment of the exo TS (6.5 D) is significantly greater than that of the endo TS (4.5 D), the influence of the solvent continuum is moderate, stabilizing the exo TS by 0.31 kcal/mol with respect to the endo one. Most of this solvent stabilization stems from electrostatic interactions (0.37 kcal/mol) whereas nonelectrostatic interactions slightly destabilize the exo TS by only 0.06 kcal/mol. Similarly, the thermodynamic exo preference is also reinforced in solution by 0.70 kcal/mol. Addition of $\Delta\Delta G_{\text{solvation}}$ to the $\Delta G_{\text{gas phase}}$ terms reduces the endo stereoselectivity of the process, the endo TS being thus 0.25 kcal/mol more stable in acetonitrile solution than the exo one in good agreement with the experimental difference of 0.20 kcal/mol.⁶ Although this coincidence between the calculated and experimental endo/exo $\Delta\Delta G_{\text{solvation}}$ values could be partially fortuitous, our results clearly show that solvent effects tend to stabilize the exo addition in contrast with the endo stabilization observed in other theoretical studies of Diels–Alder reactions in solution.²²

In conclusion, our calculations predict a small endo/exo selectivity for the prototypical Diels–Alder reaction between furan and maleic anhydride in satisfactory agreement with most of the experimental data.^{3,5,6} At the best theory level used in this work, the endo TS has ΔG values of 21.67 and 19.26 kcal/mol in the gas phase and in acetonitrile solution, respectively, only 0.56 and 0.25 kcal/mol below those of the exo isomer. According to our analyses, dispersion interactions, which stabilize the endo orientation through π – π secondary contacts, and solvent effects favoring the exo addition are the main factors governing the stereoselectivity of the process.

Acknowledgment. The authors thank CICYT, Junta de Andalucía, and the Universidad de Málaga for generous allocation of computer time at the CIEMAT, the CICA, and the SCAI, respectively. NMR kinetic measurements carried out by Dr. F. López-Ortiz (Universidad de Almería) and Dr. F. J. González (Universidad de Oviedo) are greatly appreciated. D.S. thanks F. J. González for suggesting this problem and for many stimulating discussions. The authors are much indebted to Dr. T. L. Sordo (Universidad de Oviedo) and Dr. J. J. Quirante (Universidad de Málaga) for their encouragement and comments.

Supporting Information Available: Table of energies in hartrees for all the calculations (including HF/6-31G* data); tables of BCP and Ring-CP properties for the TSs in Figure 1, figure showing the molecular geometries of endo/exo products and full geometric data for TSs and products (PDF). This material is available free of charge via the Internet at <http://pubs.acs.org>.

JA9913028

(13) No bond critical points in the MP2/6-31G* charge density were found between the C_1 – C_7 and C_4 – C_8 atoms. The C_1 – C_7 and C_4 – C_8 Mulliken overlap populations in the endo TS have values of −0.01 (MP2) and 0.00 e (B3LYP).

(14) Hoffmann, R.; Woodward, R. B. *J. Am. Chem. Soc.* **1965**, *87*, 4338.

(15) (a) Hobza, P.; Sponer, J.; Reschel, T. *J. Comput. Chem.* **1995**, *16*, 1315. (b) Pérez-Jordá, J. M.; Becke, A. D. *Chem. Phys. Lett.* **1995**, *233*, 134. (c) Kristyán, S.; Pulay, P. *Chem. Phys. Lett.* **1994**, *229*, 175.

(16) Lein, M.; Dobson, J. F.; Gross, E. K. U. *J. Comput. Chem.* **1999**, *20*, 12–22.

(17) Hobza, P.; Selzle, H. L.; Schlag, E. W. *J. Phys. Chem.* **1996**, *100*, 18790 and references therein.

(18) HF/6-31G* results are very similar to those at B3LYP/6-31G*, the endo TS being thus only 0.05 kcal/mol more stable than the exo one. This negligible HF stereoselectivity for the furan + maleic anhydride cycloaddition in the gas phase is in consonance with the proposed role played by dispersion interactions (absent in both HF and B3LYP calculations) stabilizing the endo TS.

(19) Helgaker, T.; Taylor, P. R. Gaussian Basis Sets and Molecular Integrals. In *Modern Electronic Structure Theory Part II*; Yarkony, D. R., Ed.; World Scientific: Singapore, 1995.

(20) Barone, V.; Cossi, M.; Tomasi, J. *J. Chem. Phys.* **1997**, *107*, 3210.

(21) Tomasi, J.; Persico, M. *Chem. Rev.* **1994**, *94*, 2027. (b) Tomasi, J.; Cammi, R. *J. Comput. Chem.* **1996**, *16*, 1449.

(22) Cativiela, C.; García, J. I.; Mayoral, J. A.; Salvatella, L. *Chem. Soc. Rev.* **1996**, 210.